# NUMERICAL INVESTIGATION OF THE INTERACTION BETWEEN THE ROUGHNESS AND THE TRIANGULAR OBSTRUCTIONS IN A RECTANGULAR CHANNEL

by

***Zakaria SARI HASSOUN*** [a], ***Khaled ALIANE*** [a], ***Ali AKGUL*** [b,c], ***Rabab JARRAR*** [d], ***Jihad ASAD*** [d*], ***Younes MENNI*** [e], **and** ***Hijaz AHMAD*** [f,g]

[a] MECACOMP Laboratory, Department of Mechanical Engineering, Faculty of Technology, Abou Bekr Belkaid University of Tlemcen, Tlemcen, Algeria
[b] Department of Mathematics, Art and Science Faculty, Siirt University, Siirt, Turkey
[c] Department of Electronics and Communication Engineering, Saveetha School of Engineering, SIMATS, Chennai, Tamilnadu, India
[d] Department of Physics, Faculty of Applied Science, Palestine Technical University, Kadoorie, Palestine
[e] Department of Technology, University Center Salhi Ahmed Naama, Naama, Algeria
[f] Operational Research Center in Healthcare, Near East University, Nicosia/Mersin, Turkey
[g] Section of Mathematics, International Telematic University Uninettuno, Roma, Italy

Original scientific paper
https://doi.org/10.2298/TSCI23S1365S

*The study is conducted around a heat exchanger, its channel is horizontal rectangular, its upper wall is isothermal, while its lower wall is thermally insulated, containing extended surfaces in the form of triangular obstacles attached in a staggered manner periodically. Four models of the channel with various roughnesses were compared in this study. Square, triangular Type 1, triangular Type 2, and triangular Type 3 roughnesses, which are positioned on the hot top part of the channel (absorber), downstream of the last obstacle, are examined to promote heat transfer between the absorber and the heat transfer fluid. The case of triangular roughness (Type 3) is the optimal case in terms of improved heat transfer. Moreover, it shows a significant decrease in terms of friction values.*

Key words*: numerical simulation, air-flow, triangular obstacles, rugosity, rectangular channel, heat transfer, friction, k-ε turbulent model*

## Introduction

The preparation of heat exchangers using finned ducts is among the methods commonly used by researchers. Several recent studies have focused on the optimal design of the fins and baffles for different configurations. For example, Amraoui and Aliane [1] used the CFD technique to simulate the research of fluid-flow and heat transmission in a solar channel with obstructions, fig. 1. When the air outlet temperature and the experimental findings were compared, they agreed fairly well.

Amraoui [2] used the CFX program to investigate the air-flow around a circular obstacle field in an air CSP. It creates a 3-D numerical simulation. He presented findings about heat transfer in the fluid stream, and the goal of this investigation was to demonstrate how circular obstructions affected both the fluid-flow and heat transfer in the air-flow of CSP, fig. 2.

* Corresponding author, e-mail: j.asad@ptuk.edu.ps

Amraoui [3] recently compared two different kinds of solar collectors in three dimensions. As a result, they enhanced the *Ben Slama Romdhane* solar collector by adding two air-flow tubes to promote heat transfer, fig. 3. They created a model of a flat air solar collector with transverse baffles that increase the exchange surface and create turbulence. To complete their research quickly and cheaply, they used the ANSYS simulation code.

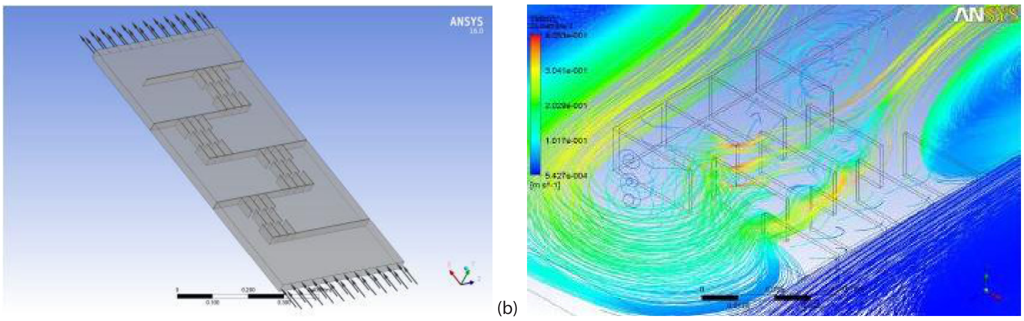


(a) (b)

**Figure 1. (a) Solar air channel with obstacles and (b) bean velocity field [1]**

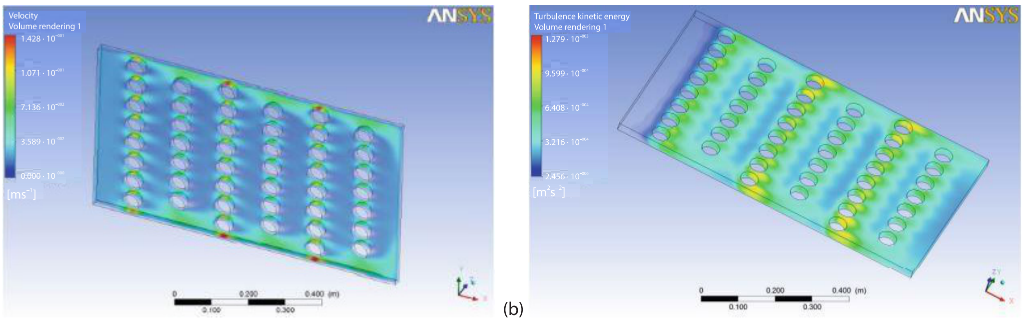


(a) (b)

**Figure 2. Hydrodynamic air fields around circular obstacles; (a) turbulent viscosity and (b) kineticenergy of turbulence [2]**

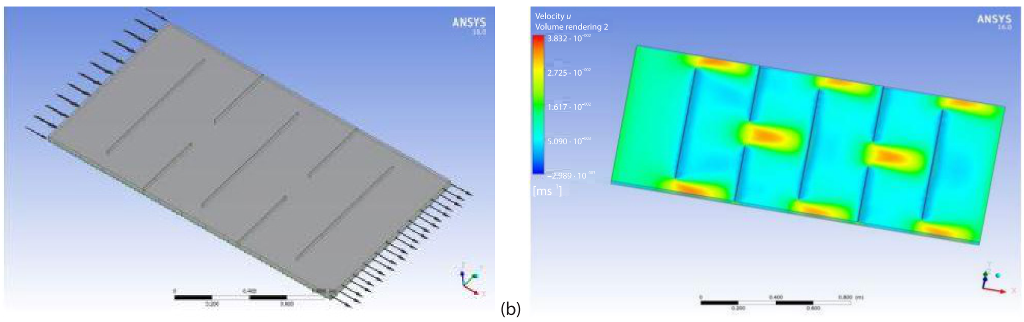


(a) (b)

**Figure 3. (a) Air CSP equipped with transverse baffles and (b) axial velocity field [3]**

In order to enhance efficiency, Amraoui and Benosman [4] also inserted square obstacles, which resulted in a very big air-flow channel in the fluid vein of the CSP to air and a sizable near-turbulence area at the site of obstacles. Due to the section's narrowing, they also notice an increase in speed between obstacles. To lessen the dead zones downstream of the obstructions, they placed the obstacles squarely. If the Reynolds number rises, they also observe a rise in the local Nusselt number and a fall in the friction factor.

On the other hand, installing small diameter wires and constructing ribs in various forms to create artificial roughness has been suggested in numerous studies as a way to enhance heat exchange system performance. For example, see Miyake *et al.* [5], Ansari and Bazargan [6], Kumar *et al*. [7], Alam *et al*. [8], Skullong *et al*. [9], and Deo *et al*. [10]. In their research, a number of dimensions have been examined for their influence. In order to investigate the effects of roughness combined with the effects of the triangular obstacles in a rectangular channel, a computational analysis of the turbulent air-flow in forced convection around deflectors mounted in staggered rows on the upper and lower walls is taken into consideration.

## Mathematical modelling

In order to improve the performance of the heat exchanger channel, rough walls are used in the presence of staggered triangular deflectors (fins and baffles), as shown in fig. 4.

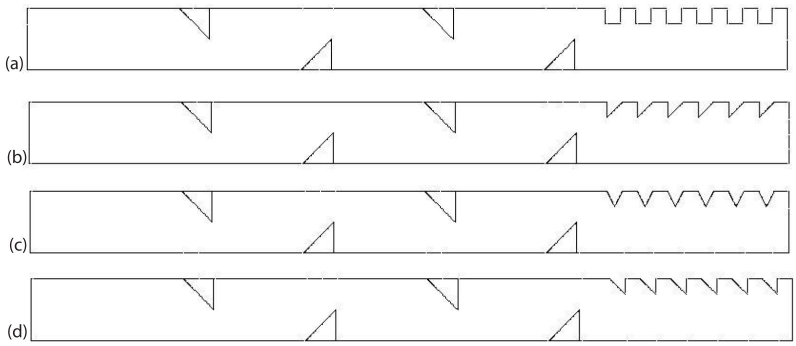


**Figure 4. Channels of different roughness, triangular in obstacles; (a) the first channel model in the presence of square roughness, (b) the second channel model in the presence of Type 1 triangular, (d) the third channel model in the presence of Type 2 triangular roughness, and (c) the fourth channel model in the presence of type 3 triangular roughness**

A comparison of the performance of four channels is made in the presence of four roughness modes, *i.e.* square, fig. 5(a), triangular Type 1, fig. 5(b), Type 2 triangular, fig. 5(c), and Type 3 triangular, fig. 5(d), as shown in fig. 5. In all the cases proposed, the roughness is present only on the hot upper wall of the channel, exactly to the right of the last obstacle. The geometry parameters for the physical model utilized is listed in tab. 1.

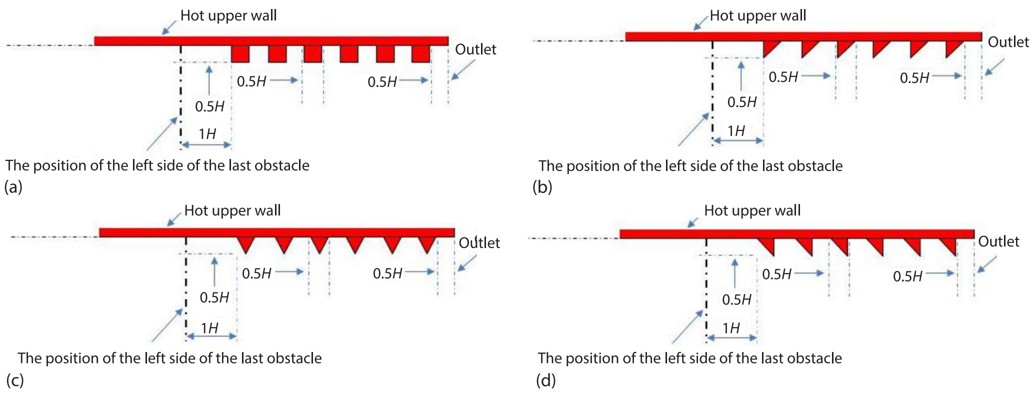


**Figure 5. Various cases of roughness shapes; (a) square roughness, (b) Type 1 triangular roughness, (c) Type 2 triangular roughness, and (d) Type 3 triangular roughness**

**Table 1. The utilised heat exchanger canal's dimensions ($H$ = 0.01 m)**

| Dimension | In terms of dimension $H$ |
|---|---|
| Channel length | 25$H$ |
| Channel height | 2$H$ |
| Hydraulic channel diameter | 2$H$ |
| Obstacle width | 1$H$ |
| Obstacle height | 1$H$ |
| Separation distance from obstacles | 3$H$ |
| Roughness width | 0.5$H$ |
| Roughness height | 0.5$H$ |
| Distance between two roughness units | 0.5$H$ |
| Distance from the channel entrance to the left side of the first obstacle | 5$H$ |
| Distance between the right side of the last obstacle and the exit from the conduit | 7$H$ |
| Distance from the right side of the last obstacle to the first roughness unit | 1$H$ |
| Distance from the right side of the last roughness unit to the exit of the channel | 0.5$H$ |

Some assumptions are taken into consideration in order to simplify the problem: the fluid's flow is stationary, the fluid is flowing in two dimensions, the fluid is turbulently flowing, the fluid-flow is Newtonian in nature, the fluid will flow without compression, the thermophysical characteristics of the used fluid and solid are taken as constants, the air fluid's velocity profile is uniform at the channel's inlet [11], and the fluid-flow is modeled using the standard $k$-$\varepsilon$ turbulence model [12].

The following conservative formulation can be used to represent the general transport equation that demonstrates the conservation of mass, momentum and energy [13]:

$$\frac{\partial}{\partial x}(\rho u\phi)+\frac{\partial}{\partial y}(\rho v\phi)=\frac{\partial}{\partial x}\left[\Gamma_\phi\frac{\partial\varphi}{\partial x}\right]+\frac{\partial}{\partial y}\left[\Gamma_\phi\frac{\partial\varphi}{\partial y}\right]+S_\varphi \tag{1}$$

where $\phi \equiv (u, v, k, \varepsilon, T)$, $u$ and $v$ is the velocity components, $k$ – the turbulent kinetic energy, $\varepsilon$ – the rate of turbulent energy dissipation, $\Gamma_\phi$ – the coefficient of diffusion, and $S_\phi$ – the source term.

The following summarizes the boundaries [11, 14, 15]:

– Inlet

$$u(0,y)=U_{\text{in}} \tag{2a}$$

$$v(0,y)=0 \tag{2b}$$

$$T(0,y)=T_{\text{in}}=300\ \text{K} \tag{2c}$$

$$k(0,y)=k_{\text{in}}=0.005U_{\text{in}}^2 \tag{2d}$$

$$\varepsilon(0,y)=\varepsilon_{\text{in}}=0.1k_{\text{in}}^2 \tag{2e}$$

– Outlet

$$P(L,y)=P_{\text{atm}} \tag{3a}$$

$$\frac{\partial \phi}{\partial x}(L,y)=0 \tag{3b}$$

– Upper wall

$$u=v=0 \tag{4a}$$

$$k=\varepsilon=0 \tag{4b}$$

$$T=T_w=375\ \text{K} \tag{4c}$$

– Lower wall

$$u=v=0 \tag{5a}$$

$$k=\varepsilon=0 \tag{5b}$$

$$\frac{\partial T}{\partial y}=0 \tag{5c}$$

By considering the results at various grid levels, a grid independent solution can be found. The results of a mesh system with a size of approximately (170 × 50) and (300 × 100) are determined to have less than 0.2% variation in heat transfer, Nusselt number. The system of mesh of (170 × 50) cells with high resolution near the walls was selected for the numerical situation taking into account both convergence rate and solution accuracy. The SIMPLE algorithm served as the foundation for the numerical approach used in this investigation. The finite volume approach with second-order upwind (SOU) and QUICK schemes are used to discretize the conservation equations [16, 17]. The validation of the model is detailed in our recent study under the supervision of Prof. Khaled Aliane [18].

## Results and analysis

Figure 6 represents the distribution of the average speed as a function of the shape of the roughness (square roughness and triangular roughness) in the presence of triangular obstacles. In the case of square roughness, the average velocity is negligible due to the unprofiled deformation of the driving surface. In the case of a triangular roughness (Type 1), the average speed is low at the beginning of the roughness, because the profile tracking downstream of the roughness. In the case of a triangular roughness (Type 2), the average velocity is relatively high, because the flow profiling discontinuity with the roughness. In the case of a triangular roughness (Type 3), the average speed has a large value.

Figure 7 shows the temperature distribution throughout the region studied for the four models proposed for roughness and in the presence of fins and triangular baffles. The temperature is very high in the areas close to the obstacles and the absorber as well as the asperities of the roughness. Adding roughness gives an improvement to the exit of the channel. In the case of square roughness, the fluid temperature field has low cooling efficiency, due to poor air re-circulation in the center of the roughness. In the case of the triangular roughness (Type 1), the channel has a good cooling, due to the insertion of the air-flow in the roughness. In the case of the triangular roughness (Type 2), the temperature field has a good agitation with the area, because the good curvature of the roughness. In the case of a triangular roughness (Type 3), the temperature field has perfect cooling, because the best straightening of the heat flux by this roughness.

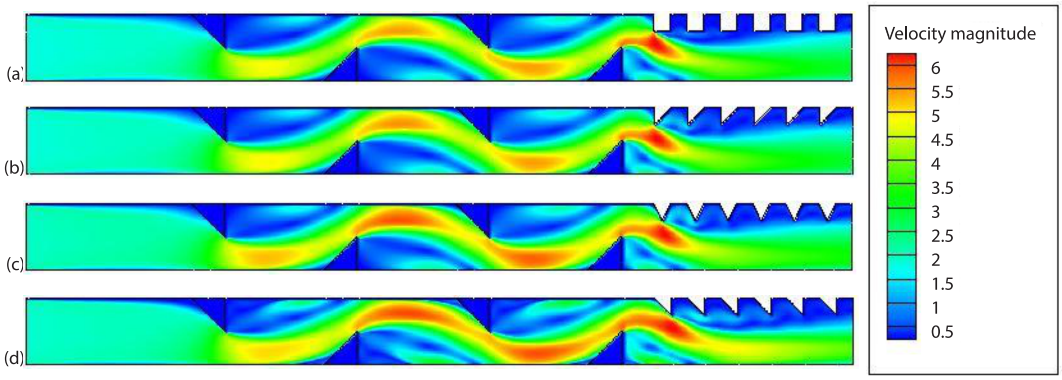


**Figure 6. Contour plots of mean velocity fields in various roughnesses, Re = 2500; (a) square roughness, (b) triangular roughness (Type 1), (c) triangular roughness (Type 2), and (d) triangular roughness (Type 3)**

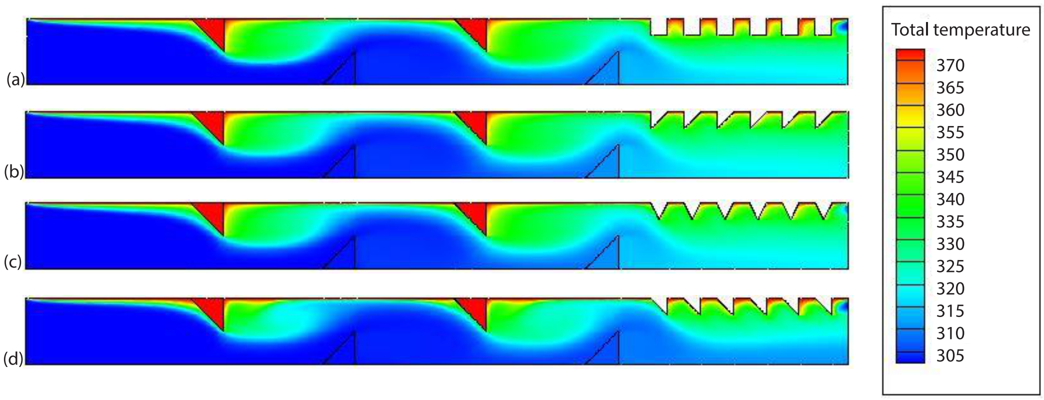


**Figure 7. Contour plots of temperature fields in various roughnesses, Re = 2500; (a) square roughness (b) triangular roughness (Type 1), (c) triangular roughness (Type 2), and (d) triangular roughness (Type 3)**

Figure 8 gives the variations of the values of $Nu/Nu_0$ as a function of the Reynolds number for the various cases of roughness examined for the air duct with triangular fins. For all cases of roughness, the mean Nusselt number increases with increasing Reynolds number. High speed gives high convection. The figure shows that the average Nusselt number has a high value in the case of a triangular roughness (Type 3), due to the good guidance of the flow. For the case of triangular roughness (Type 2), the Nusselt number is reduced, due to the uniform separation of the flow. In the case of a triangular roughness (Type 1), the Nusselt number is low, because the roughness of the attack surface is straight. In the case of square roughness, the Nusselt number is negligible, due to poor fluid re-circulation. In the absence of roughness, a very significant decrease in the Nusselt values, because the exchange surface is low.

Figure 9 presents the evolution of the average ratio ($f/f_0$) as a function of the Reynolds number which varies between 2500 and 10000, for four different forms of roughness, *i.e.*, square and triangular (Types 1-3).

The average coefficient of friction increases with increasing Reynolds number. The figure shows that the average coefficient of friction has a large value in the case of square roughness, because there is a large contact surface. For the case of triangular roughness (Type 1), the

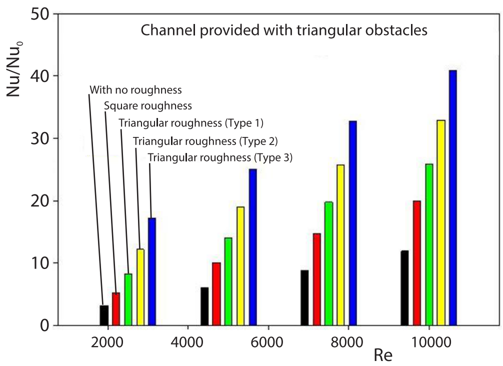


**Figure 8. Normalized average Nusselt number ($Nu/Nu_0$) as a function of the Reynolds number in various roughnesses**

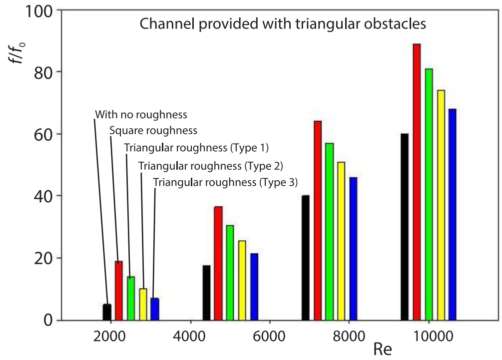


**Figure 9. Normalized average coefficient of friction ($f/f_0$) as a function of the Reynolds number in various roughnesses**

coefficient of friction is reduced, because the roughness is perpendicular to the flow direction. In the case of a triangular roughness (Type 2), the coefficient of friction is lower, due to the low disturbance of the flow. In the case of a triangular roughness (Type 3), the coefficient of friction is lowered, because the flow resistance is low. In the case without roughness, the coefficient of friction is low, because there is no roughness which hinders the passage of the flow.

## Conclusion

The present analysis is focused on a heat exchanger channel with a rectangular configuration, an isothermal top wall, a thermally insulated bottom wall, and extended surfaces in the form of staggered triangular obstructions. In this study, four channel types with different models of roughness were compared. In order to encourage heat transmission between the hot surfaces and the heat transfer fluid, square, triangular Type 1, triangular Type 2, and triangular Type 3 roughnesses that are positioned on the heated top part of the channel (absorber), downstream of the final obstacle, are explored. For enhanced heat transfer, the situation with triangular roughness (Type 3) is the best. Additionally, it exhibits a notable reduction in friction levels.

## Acknowledgment

The authors Rabab Jarrar and Jihad Asad would like to thank Palestine Technical University- Kadoorie for supporting them financially

## References

[1] Amraoui, M. A., Aliane, K., The 3-D Analysis of Air-flow in a Flat Plate Solar Collector, *Periodica Polytechnica Mechanical Engineering*, *62* (2018) 2, pp. 126-135
[2] Amraoui, M. A., *Numerical Study of an Air-flow in a Flat Plate Air Solar Collector with Circular Obstacles*, In International Conference in Artificial Intelligence in Renewable Energetic Systems, Springer, Cham, Switzerland, 2020, pp. 839-846
[3] Amraoui, M. A., The 3-D Numerical Simulation of a Flat Plate Solar Collector with Double Paths, *Int. Journal of Heat and Technology*, *39* (2021) 4, pp. 1087-1096
[4] Amraoui, M. A., Benosman, F., Numerical Modelling of a Flat Air Solar Collector Fitted with Obstacles, *Proceedings*, E3S Web of Conferences, 2021, Vol. 321, 04016
[5] Miyake, Y., *et al*., Direct Numerical Simulation of Rough-Wall Heat Transfer in A Turbulent Channel Flow, *Int. Journal of Heat and Fluid-Flow*, *22* (2001) 3, pp. 237-244
[6] Ansari, M., Bazargan, M., Optimization of Flat Plate Solar Air Heaters with Ribbed Surfaces, *Applied Thermal Engineering*, *136* (2018), May, pp. 356-363

[7] Kumar, R., *et al.*, A parametric Analysis of Rectangular Rib Roughened Triangular Duct Solar Air Heater Using Computational Fluid Dynamics, *Solar Energy*, *157* (2017), Nov., pp. 1095-1107
[8] Alam, T., *et al.*, Heat Transfer Enhancement in Solar Air Heater Duct with Conical Protrusion Roughness Ribs, *Applied Thermal Engineering*, *126* (2017), Nov., pp. 458-469
[9] Skullong, S., *et al.*, Heat Transfer Augmentation in a Solar Air Heater Channel with Combined Winglets and Wavy Grooves on Absorber Plate, *Applied Thermal Engineering*, *122* (2017), July, pp. 268-284
[10] Deo, N. S., *et al.*, Performance Analysis of Solar Air Heater Duct Roughened with Multigap V-Down Ribs Combined with Staggered Ribs, *Renewable Energy*, *91* (2016), June, pp. 484-500
[11] Demartini, L. C., *et al.*, Numeric and Experimental Analysis of The Turbulent Flow Through a Channel with Baffle Plates, *Journal of the Brazilian Society of Mechanical Sciences and Engineering*, *26* (2004), 2, pp. 153-159
[12] Launder, B. E., Spalding, D. B., The Numerical Computation of Turbulent Flow, *Computer Methods in Applied Mechanics and Engineering*, *3* (1974), 2, pp. 269-289
[13] Yang, Y. T., Hwang, C. Z., Calculation of Turbulent Flow and Heat Transfer in a Porous-Baffled Channel, *Int. Journal of Heat and Mass Transfer*, *46* (2003), 5, pp. 771-780
[14] Siddiqui, M. K., Heat Transfer Augmentation in a Heat Exchanger Tube Using a Baffle, *Int. Journal of Heat and Fluid-Flow*, *28* (2007), 2, pp. 318-328
[15] Dutta, P., Hossain, A., Internal Cooling Augmentation in Rectangular Channel Using Two Inclined Baffles, *Int. Journal of Heat and Fluid-Flow*, *26* (2005), 2, pp. 223-232
[16] Patankar, S. V., *Numerical Heat Transfer and Fluid-Flow*, McGraw-Hill, New York, USA, 1980
[17] Leonard, B. P., Mokhtari, S., Ultra-Sharp Non-Oscillatory Convection Schemes for High-Speed Steady Multidimensional Flow, NASA TM 1-2568, NASA Lewis Research Center, Cleveland, O., USA, 1990
[18] Menni, S., Belabbaci, F., Study of the Dynamic Structure of Turbulent Flow around an Obstacle: Effect of Thermal Stratification, Etude des écoulements turbulents autours d'un obstacle: effet de la rugosité couplé à l'inclinaison (in French), M. Sc. thesis, Université Aboubakr Belkaïd-Tlemcen, 2022

Paper submitted: May 16, 2022
Paper revised: June 4, 2022
Paper accepted: June 10, 2022